Mutational Analysis of Amino Acid Residues Involved in Argininosuccinate Lyase Activity in Duck δ II Crystallin†

Anita R. Chakraborty,‡,§ Alan Davidson,§,|| and P. Lynne Howell*,‡,§

Structural Biology and Biochemistry, Research Institute, Hospital for Sick Children, 555 University Avenue, Toronto, M5G 1X8 Ontario, Canada, and Departments of Biochemistry and Molecular and Medical Genetics, Faculty of Medicine, University of Toronto, Medical Sciences Building, Toronto, M5S 1A8 Ontario, Canada

Received September 4, 1998; Revised Manuscript Received November 4, 1998

ABSTRACT: δ-Crystallins are the major structural eye lens proteins of most birds and reptiles and are direct homologues of the urea cycle enzyme argininosuccinate lyase. There are two isoforms of δ-crystallin, δ I and δ II, but only δ II crystallin exhibits argininosuccinate lyase (ASL) activity. At the onset of this study, the structure of argininosuccinate lyase/δ II crystallin with bound inhibitor or substrate analogue was not available. Biochemical and X-ray crystallographic studies had suggested that H162 may function as the catalytic base in the argininosuccinate lyase/δ II crystallin reaction mechanism, either directly or indirectly through the activation of a water molecule. The identity of the catalytic acid was unknown. In this study, the argininosuccinate substrate was modeled into the active site of duck δ II crystallin, using the coordinates of an inhibitor-bound *Escherichia coli* fumarase C structure to orient the fumarate moiety of the substrate. The model served as a means of identifying active site residues which are positioned to potentially participate in substrate binding and/or catalysis. On the basis of the results of the modeling, site-directed mutagenesis was performed on several amino acids, and the kinetic and thermodynamic properties of each mutant were determined. Kinetic studies reveal that five residues, R115, N116, T161, S283, and E296, are essential for catalytic activity. Determination of the free energy of unfolding/refolding of wild-type and mutant δ II crystallins revealed that all constructs exhibit similar thermodynamic stabilities. During the course of this work, the structure of an inactive δ II crystallin mutant with bound substrate was solved [Vallee et al. (1999) *Biochemistry 38,* 2425−2434], which has allowed the kinetic data to be interpreted on a structural basis.

Crystallins are the major structural proteins of the vertebrate eye lens, where they constitute 80−90% of the total soluble lenticular protein (*2*). They are a diverse family of proteins which function in maintaining the physical properties of the lens such as its transparency and refractive index (*3*−*6*). They are also speculated to protect the lens from UV[1] and oxidative damage (*7*). Crystallin family members have been classified according to their species distribution. The ubiquitous crystallins (α, β, and γ) are incident in all vertebrate species, while the taxon-specific variety (δ, ε, λ, τ, etc.) are expressed in a species-dependent manner. The ubiquitous crystallins are believed to have evolved much earlier than the taxon-specific class (*8*). Crystallins are not renewed, and therefore they must maintain their structural and functional integrity throughout the lifetime of an organism. Rather than evolving as highly specialized structural proteins, as might have been expected given their essential lenticular functions, many of the taxon-specific crystallins are direct homologues of house-keeping enzymes (*9*−*11*). House-keeping enzymes have been recruited to the eye lens by a phenomenon called *gene sharing*. This is a process whereby an enzyme is recruited, without any prior gene duplication, to a new structural eye lens role (*9*, *11*, *12*). Recruitment presumably favors those enzymes which are thermodynamically stable and able to accumulate to high physiological concentrations without aggregating (*8*, *10*, *13*). Following recruitment to the lens, gene duplication may then occur; however, this is not necessary for the evolution of the enzyme's new structural role (*11*, *14*−*16*). The genetic mechanisms driving lens-specific overexpression of enzymes/crystallins are not understood but presumably involve the modification of promoter and/or enhancer elements. The enzyme/crystallin is expressed at low levels in many tissues to fulfill its enzymatic role while it is simultaneously overexpressed in the lens as a crystallin.

δ-Crystallin is the major lenticular protein in avian and some reptilian species, displacing γ-crystallin, which is a principal constituent of mammalian lenses (*17*). δ-Crystallin

† Supported by a grant from the Medical Research Council of Canada to P.L.H.

* Corresponding author: (416) 813-5378 (phone); (416) 813-5022 (fax), howell@sickkids.on.ca (e-mail).

‡ Hospital for Sick Children.

§ Department of Biochemistry, University of Toronto.

|| Department of Molecular and Medical Genetics, University of Toronto.

[1] Abbreviations: A_{600}, absorbance at 600 nm; ASL, argininosuccinate lyase; CD, circular dichroism; cDNA, complementary deoxyribose nucleic acid; DNA, deoxyribose nucleic acid; EDTA, ethylenediaminetetraacetate; GdnHCl, guanidine hydrochloride; IPTG, isopropyl thiogalactoside; K_m, Michaelis constant; OD, optical density; PMSF, phenylmethanesulfonyl fluoride; rms, root mean square; SDS−PAGE, sodium dodecyl sulfate−polyacrylamide gel electrophoresis; TPCK, L-1-tosylamido-2-phenylethyl chloromethyl ketone; UV, ultraviolet; V_{max}, maximal velocity; wt, wild type.

10.1021/bi982150g CCC: $18.00
Published on Web 02/05/1999

	114 121	159 168	282 296
DDC II	**S**R**ND**Q**V**V**T**	GY**THLQ**K**A**Q**P**	**GSS**L**MP**Q**KK**N**P**DSL**E**
DDC I	**S**R**N**EQ**V**V**T**	GY**THLQ**K**A**Q**P**	**GSS**L**MP**Q**KK**N**P**DSL**E**
CDC II	**S**R**ND**Q**V**V**T**	GY**THLQ**K**AL**P**	**GSS**LL**P**Q**KK**N**P**DSL**E**
CDC I	**S**R**N**EQ**V**V**T**	GY**THLQ**K**AL**P**	**GSS**LL**P**Q**KK**N**P**DSL**E**
ASL_H	**S**R**ND**Q**V**V**T**	GY**THLQ**R**A**Q**P**	**GSS**L**MP**Q**KK**N**P**DSL**E**
ASL_Y	**S**R**ND**Q**V**V**T**	GY**THLQ**R**A**Q**P**	**GSS**L**MP**Q**KK**N**A**DSL**E**
FUM_BS	**S**S**ND**TFP**T**	GR**THLQ**D**AT**P**	**GSS**I**MP**G**K**V**NP**TQS**E**
FUM_EC	**S**S**ND**VFP**T**	GR**THLQ**D**AT**P**	**GSS**I**MP**G**K**V**NP**TQC**E**
FUM_H	**S**S**ND**TFP**T**	GR**THT**Q**D**A**V**P**	**GSS**I**MP**G**K**V**NP**TQC**E**
ASP_BS	**SQND**VFP**T**	GR**THLQ**D**A**V**P**	**GSS**I**MP**G**K**V**NP**VMA**E**
ASP_EC	**ST**N**D**AYP**T**	GR**T**Q**LQ**D**A**V**P**	**GSS**I**MP**A**K**V**NP**VVP**E**
ADL_BS	TST**D**V**V**D**T**	GR**TH**GVH**AE**P	**GSS**A**MP**Y**K**R**NP**MRS**E**
ADL_H	TSCYVGDN	GS**THF**Q**PA**QL	**GSS**A**MP**Y**K**R**NP**MRS**E**
ADL_EC	TSE**D**INNL	SR**TH**G**Q**P**AT**P	**GSS**T**MP**H**K**V**NP**IDF**E**
CMLE_PP	TSQ**D**AMD**T**	GR**T**W**LQ**H**AT**P	**GSS**T**MP**H**K**R**NP**VGAA
CONSENSUS	**S-ND-V-T**	**G-THLQ-A-P**	**GSS-MP-K-NP---E**

FIGURE 1: Sequence alignment of the three highly conserved regions across the ASL/δ crystallin superfamily. According to the duck δ II numbering scheme, conserved region 1 includes residues 114−121; conserved region 2, residues 159−168; and conserved region 3, residues 282−296. Key to the sequence alignments: DDC II, duck δ II crystallin; DDC I, duck δ I crystallin; CDC II, chicken δ II crystallin; CDC I, chicken δ I crystallin; ASL_H, human argininosuccinate lyase; ASL_Y, yeast argininosuccinate lyase; FUM_BS, *B. subtilis* fumarase C; FUM_EC, *E. coli* fumarase C; FUM_H, human fumarase C; ASP_BS, *B. subtilis* aspartase; ASP_EC, *E. coli* aspartase; ADL_BS, *B. subtilis* adenylosuccinate lyase; ADL_H, human adenylosuccinate lyase; ADL_EC, *E. coli* adenylosuccinate lyase; CMLE_PP, *P. putida* 3-carboxy-*cis*,*cis*-muconate lactonizing enzyme.

imparts a soft, flexible property to the lens (*18*), which allows for the long-range accommodation characteristic to the eyesight of birds. δ-Crystallin is homologous to the enzyme argininosuccinate lyase (ASL) (EC 4.3.2.1). After recruitment of the enzyme to an eye lens function, gene duplication occurred, resulting in the δ I and δ II isoforms. Although there exists 88−94% amino acid sequence identity between the δ I and δ II proteins from various species (*12*, *19*, *20*), only δ II crystallin has retained ASL activity. ASL is expressed predominantly in the livers of ureotelic species where it participates in the urea cycle by catalyzing the reversible hydrolysis of argininosuccinate to arginine and fumarate. ASL is also ubiquitously expressed across all species where it participates in arginine biosynthesis (*21*). ASL/δ-crystallin belongs to a superfamily of enzymes that includes class II fumarase (*22*), L-aspartase (*23*, *24*), adenylosuccinate lyase (*25*), and 3-carboxy-*cis*,*cis*-muconate lactonizing enzyme (*26*). Each of these enzymes is biologically active as a 200 kDa homotetramer and catalyzes the formation of fumarate via a β-elimination reaction involving cleavage of a C_α−N or C_α−O bond. Structures of four of the six superfamily members have been solved by X-ray crystallographic techniques (*18*, *27*−*31*) and reveal that each shares a common protein fold. Each monomer contains three domains comprised primarily of α-helices [see Figure 1 (*1*)]. The monomers oligomerize with 222 symmetry to form a tetramer with the central helices of each monomer associating to form a 20-helix core. Although the overall sequence homology across all superfamily members is quite low (approximately 15%), there are three highly conserved regions of amino acid residues (Figure 1). The structural studies on turkey δ I crystallin (*18*) revealed that while these three conserved regions are spatially remote from one another in the tertiary structure of the monomer, they cluster together as a result of quaternary assembly of the protein to form four active sites, one at each "corner" of the enzyme. Each active site cleft is comprised of one conserved region from three of the four subunits that make up the tetrameric enzyme. The location of the active site was confirmed by the structure of *Escherichia coli* fumarase C complexed with an inhibitor (*30*).

The ASL reaction proceeds by a general acid−base mechanism which is initiated by proton abstraction at the C_β position of argininosuccinate to form a carbanion intermediate. Subsequent proton donation at the guanidinium nitrogen is accompanied by cleavage of the labile C_α−N bond to release the products, arginine and fumarate. Inhibitor-bound *Escherichia coli* fumarase C structures (*30*, *31*) as well as chemical modification and site-directed mutagenesis of ASL and δ II crystallin (*32*−*34*) have implicated histidine 162 as being involved either directly in base catalysis or indirectly through the activation of a water molecule. The identity of the proton donor remains unknown, although lysine 289, serine 114, histidine 162, and an active site water molecule have all been suggested as possible candidates (*18*, *30*, *31*). In this study, duck δ II crystallin was used as a structural model to identify those residues involved in acid catalysis and substrate binding in the ASL/δ II reaction mechanism. At the beginning of this study there was no structure of δ II crystallin/ASL with bound inhibitor or substrate analogue available, and therefore the argininosuccinate substrate was modeled into the δ II active site. Coordinates of *E. coli* fumarase C with citrate bound in the active site (*31*) were used as a structural model for comparative purposes in order to orient the fumarate moiety of the substrate in the active site. These modeling studies served as a basis for identifying amino acid residues which may either putatively function as the acid catalyst in the reaction mechanism or be involved in substrate binding. The roles of these residues in catalysis were subsequently examined by site-directed mutagenesis and quantitation of the kinetic and thermodynamic properties of the mutant enzymes.

MATERIALS AND METHODS

Modeling the Substrate into the δ II Active Site. To identify residues which may participate in the catalytic mechanism of δ II crystallin, the coordinates of a mutant H110N δ II structure (Turner and Howell, manuscript in preparation)

Table 1: Primers Used To Construct δ II Crystallin Mutants[a]

mutant	primer sequence (5′ to 3′)
E296Q	P-GAA GAA CCC TGA TAG CCT GcA gCT GAT CCG C (*Pvu*II)
N116L	P-CCG GAA GAA Gtc Gac tgG ATC AGG TTG TGA CTG (*Sal*I)
R113N	P-GCA CAC CGG AAa ctc gAG GAA TGA TCA G (*Xho*I)
R115N	P-GCA CAC CGG AcG ttc gAa tAA TGA TCA GG (*Bsp*1191)
S114A	P-CAC ACC GGA AGA gct cGG AAT GAT CAG (*Sac*I)
S283A	P-GCA CTG GCg cCA GCC TGA TGC CTC AGA AG (*Kas*I)
S284A	P-CAC TGG CAG Cgc tCT GAT GCC TCA GAA G (*Eco*47III)
T161V	P-GCC TGG CTA tgt aCA CCT GCA GAA GGC CC (*Bsp*14071)
Y323F	P-GGA CTT CCA tca ACg TtC AAC AAG GAC C (*Psp*14061)
Y323I	P-GAC TTC CAA GtA Cta tCA ACA AGG AC (*Sca*I)

[a] All mutagenic primers were phosphorylated at their 5′ ends. Mismatched bases which constitute the mutagenic replacements are shown in lower case. Restriction endonuclease sites have been underlined and annotated to indicate the introduction of a new site into the template sequence.

were superimposed with those of an inhibitor-bound *E. coli* fumarase C structure (*31*) using the program LSQMAN (*35*−*37*). Superposition of the 20-helix core (in δ II corresponding to residues 115−151, 171−196, 239−265, 293−314, and 330−354) of each tetrameric structure yielded a rms difference separation of 1.6 Å between corresponding C_α positions. The coordinates of argininosuccinate were built using the program Quanta (*38*) and subsequently modeled into the δ II active site using the program TURBO−FRODO (*39*). The fumarate moiety of argininosuccinate was oriented to occupy a position similar to that of the citrate inhibitor molecule bound in the active site of *E. coli* fumarase C. In general, active site residues located within an 8 Å radius of the substrate were chosen as candidates for site-directed mutagenesis.

Site-Directed Mutagenesis. Site-directed mutants of duck (*Anas platyrhonchos*) δ II crystallin were constructed using the Unique Site Elimination Mutagenesis kit from Pharmacia (*40*−*42*). Wild-type duck δ II cDNA was subcloned from pET-3d (a gift of Dr. W. E. O'Brien) into the *Xba*I and *Hind*III sites of the pUC-19 vector (Pharmacia), which subsequently served as the template for all mutagenesis reactions. Table 1 lists the mutagenic primers used in the construction of each mutant. In addition to the mutation of the desired codon(s), each oligonucleotide primer was designed to introduce a new restriction endonuclease site into the template sequence. This site served as a tool for the selection of positive mutants. Mutated cDNA was then subcloned into the *Xba*I and *Hind*III sites of the pET-3d vector in frame with a C-terminal six-histidine tag. Preliminary screening of positive mutants was accomplished by restriction enzyme mapping and was confirmed by DNA sequencing over the area containing the mutation.

Protein Expression and Purification. DNA was transformed into *E. coli* strain BB101, the genotype of which is *ara* Δ(*lac proAB*) Δ*slyD* (*kan*^{r}) *nalA argEam rif thi* F′[*lacI*^{q} *proAB*$^+$] (λDE3). The *slyD* deletion prevents the expression of a 21 kDa histidine-rich *E. coli* protein that binds strongly to the cobalt affinity resin used to purify the proteins studied in these experiments. A single colony was used to inoculate two 5 mL LB cultures which were incubated overnight at 37 °C. Overnight growths were then diluted in 1 L of LB, and the culture was grown at 37 °C to an OD_{600} of 0.5−0.6 at which point protein expression was induced by the addition of IPTG to a final concentration of 1 mM. Cells were harvested 3−4 h post-induction by centrifugation at 8000 rpm for 25 min at 4 °C in a Beckman J2-21 centrifuge (JA-10.5 rotor). The supernatant was decanted, and the cells were stored at −20 °C until required. Frozen cells from 1 L of culture were resuspended in 12.5 mL of column buffer consisting of 10 mM Tris-HCl, pH 8.0, supplemented with 1 mM PMSF and 10 μg/mL TPCK, and sonicated for a total of 3.5 min with 30 s pulses followed by 60 s of cooling on ice. The sample was centrifuged at 14 000 rpm for 30 min at 4 °C in a Beckman J2-21 centrifuge (JA-20 rotor). The soluble fraction was decanted and stored on ice while the pellet was resuspended in column buffer, sonicated, and centrifuged as in the previous step. The pooled (25 mL) lysates were subsequently passed through a Millipore Millex-HV 0.45 μM filtration unit. The lysate was divided in half and each half mixed with 5 mL of Talon Metal Affinity Resin (Clontech) that had been previously equilibrated with column buffer. Binding of the protein was achieved by rotating the samples for 30 min at 4 °C. The samples were centrifuged at 1500 rpm for 5 min at room temperature in a Beckman GS-6KR centrifuge (GA-10 rotor), and the supernatant was discarded. Each pellet was then washed in 50 mL of column buffer and rotated for an additional 10 min at room temperature. The samples were centrifuged as in the previous step, the supernatant was discarded, and the final wash step was repeated as before. The washed resin was then transferred to a column, and 30 mL of column buffer containing 15 mM imidazole was passed through under gravity flow. The protein was eluted with 15 mL of 10 mM Tris-HCl, pH 7.5, 100 mM NaCl, and 100 mM imidazole and the eluate collected in two 7.5 mL fractions. The first eluted fraction contained most of the protein, as determined by relatively high OD_{280} readings as well as the presence of a band of the expected molecular mass of 50 kDa on an SDS−PAGE gel (data not shown). The first eluted fraction was dialyzed overnight at 4 °C into 10 mM Tris-HCl, pH 7.5, and 1 mM EDTA. This protocol yielded approximately 25 mg of about 95% pure protein from 1 L of bacterial culture.

Enzyme Assay. The enzymatic activity of wild-type and mutant δ II crystallins was determined spectrophotometrically. Reaction mixtures were prepared by diluting a stock solution of sodium argininosuccinate (Sigma-Aldrich) to a final concentration of 0.02−8.0 mM in 10 mM Tris-HCl, pH 7.5. For the E296Q mutant the concentration range of substrate used was 0.01−0.18 mM. Reactions were initiated by the addition of 20−50 μg of enzyme. After brief mixing, the enzymatic activity was monitored as a function of the appearance of fumarate at 240 nm ($\epsilon = 2.44\ mM^{-1}\ cm^{-1}$) on a Milton Roy 3000 spectrophotometer. All active enzymes displayed Michaelis−Menten kinetics. Data points were collected in triplicate and initial velocities fit to the Lineweaver−Burk equation in order to determine the kinetic parameters K_m and V_{max}.

Circular Dichroism Spectroscopy. The CD spectra of wild-type and mutant δ II crystallins were measured on an AVIV circular dichroism Model 62A DS spectrometer. A 0.2 μM solution of protein in 10 mM Tris-HCl, pH 7.5, and 1 mM EDTA was scanned from 200 to 270 nm in a cell with a path length of 0.1 cm. The spectra were acquired using 1 nm steps and an integration time of 1 s. To compare their relative thermodynamic stabilities, the proteins were reversibly denatured in guanidine hydrochloride (Pierce). A 0.2 μM solution of enzyme in 10 mM Tris-HCl, pH 7.5, and 1 mM EDTA was titrated from 0 to 6.9 M GdnHCl and 7.0 to 0.1 M GdnHCl for the denaturation and renaturation reactions, respectively. Reactions were performed at 25 °C in a cell with a path length of 1 cm. After each addition of titrant the sample was mixed for 60 s prior to obtaining the spectra. Unfolding/refolding was monitored as a function of CD signal at 222 nm. Each data point was taken as the average of 301 observations measured over 30 s with an integration time of 0.1 s. The denaturation/renaturation curve of δ II is biphasic, i.e., the structural transition from tetramer to monomer occurs via an intermediate species. From analytical ultracentrifugation studies on human ASL, the intermediate has been identified as a dimer (*43*). Wild-type and mutant denaturation data were fit to a tetramer ↔ 2 dimer ↔ 4 monomer equilibrium model using the numerical solver BIOEQS (*44*, *45*). Gibb's free energies for the first (tetramer ↔ dimer) and second (dimer ↔ monomer) transitions for each of the unfolding and refolding reactions were quantitated using this method.

RESULTS

Selection of Mutagenic Targets. The modeling of the substrate, argininosuccinate, into the active site of the protein identified the following residues as being within 8 Å of the substrate: R113, S114, R115, N116, T161, E296, Y323, H91, V119, T281, N291, D293, and K325. We have concentrated on the first seven residues listed as they were either in closest proximity to the modeled substrate (<4 Å) or contained functional groups that may potentially function in acid catalysis. S283 and S284 were additional candidates because these two residues are invariant across all superfamily members (Figure 1) and are located on a conformationally flexible loop (the 280's loop) that is thought to be important for catalysis. E296 is speculated to participate in a charge-relay with H162 (*30*), and therefore this residue was mutagenized to demonstrate its importance in the context of ASL/δ II crystallin. In designing the δ II mutants, amino acid substitutions were kept as isosteric as possible in order to minimize any structural variation that may occur in the active site as a consequence of the mutation.

Assessing Conformational Integrity Using Circular Dichroism. The CD spectra of wild-type and mutant δ II crystallins were measured from 200 to 270 nm. All spectra displayed minima at 208 and 222 nm as is characteristic of proteins comprised of largely α-helical secondary structure (Figure 2). The superposition of all spectra reveals that, with the exception of R115N and E296Q, mutations introduced into the wild-type δ II sequence did not significantly alter the secondary structural elements of the protein. The R115N and E296Q mutants appear to have lost 20−30% of their α-helicity in comparison to wild-type δ II crystallin.

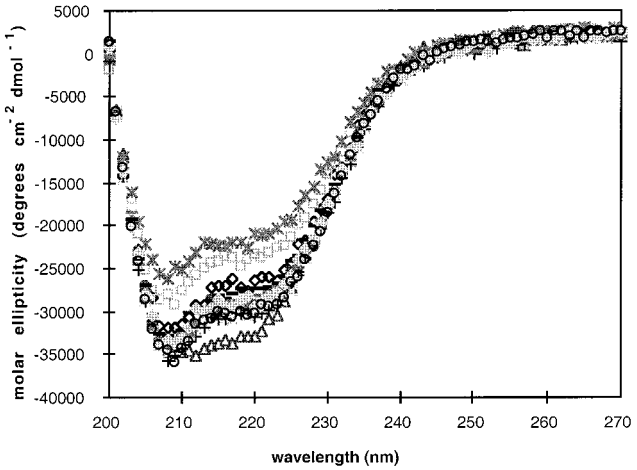

FIGURE 2: Circular dichroism spectra of wild-type, and mutant δ II crystallins. Protein (0.2 μM) was scanned from 200 to 270 nm, and the resulting spectra were superimposed. Key to the plot: (◇) wild-type δ II crystallin; (□) E296Q; (△) N116L; (×), R113N; (★), R115N; (●), S114N; (+) S283A; (—) S284A; (−) T161V; (◆), Y323F; (○), Y323I.

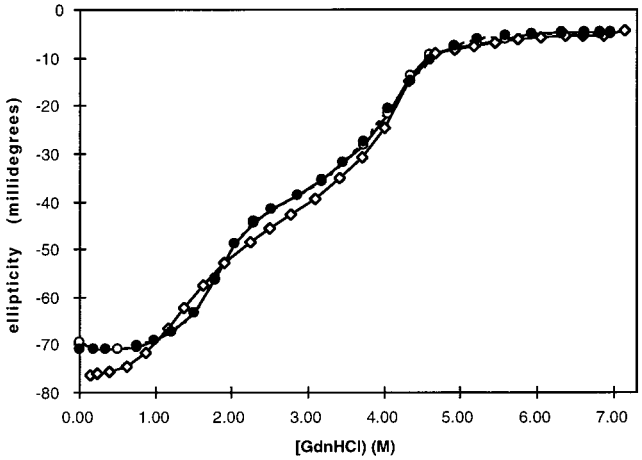

FIGURE 3: Superposition of the experimental denaturation (○) and renaturation (◇) curves along with the modeled data for the denaturation reaction (●) of wild-type δ II crystallin. Unfolding was monitored as a function of the circular dichroism signal at 222 nm. In the denaturation reaction the sample was titrated from 0 to 6.9 M GdnHCl. For the renaturation reaction the titration was performed from 7 to 0.1 M GdnHCl. The denaturation data were fit to a biphasic transition using the program BIOEQS. The residuals between the modeled and experimental observations at each data point were small and random (data not shown).

Global Fitting of Reversible GdnHCl Denaturation Using BIOEQS. Equilibrium binding curves monitored by CD reveal that wild-type and mutant δ II crystallins are reversibly denatured in GdnHCl. The shapes of both the denaturation (0.0−6.9 M GdnHCl) and renaturation (7.0−0.1 M GdnHCl) curves illustrate that the structural transition from folded tetramer to unfolded monomer is biphasic in nature (Figure 3). The forward and reverse denaturation curves are superimposable, implying that this unfolding reaction is fully reversible. Analytical ultracentrifugation studies on human ASL have identified the intermediate species as a dimer (*43*). Given this three-state transition model, two Gibb's free energies (ΔG°) can be associated with each denaturation/renaturation reaction. ΔG°_1 and ΔG°_2 represent the free energies of the tetramer ↔ 2 dimer and 2 dimer ↔ 4 monomer equilibria, respectively. Global fitting of GdnHCl

Table 2: Kinetic Parameters for Wild-Type and Mutant δ II Crystallins

enzyme	V_{max} (μmol min^{-1} mg^{-1})	K_m (mM)	k_{cat} (s^{-1})	k_{cat}/K_m (M^{-1} s^{-1})
wt δ II	1.5 ± 0.2	0.07 ± 0.01	4.9 ± 0.6	(7.4 ± 1.8)E^4
S114A	0.73 ± 0.04	0.09 ± 0.01	2.42 ± 0.07	(2.6 ± 0.1)E^4
R113N	0.20 ± 0.01	0.03 ± 0.01	0.62 ± 0.01	(2.3 ± 0.1)E^4
S284A	0.03 ± 0.01	0.02 ± 0.01	0.12 ± 0.01	(5.3 ± 0.6)E^3
Y323F	1.3 ± 0.1	1.7 ± 0.1	4.3 ± 0.1	(2.5 ± 0.1)E^3
E296Q	1.5 ± 0.1 E^{-2}	(5.8 ± 0.1)E^{-3}	(5.3 ± 0.2)E^{-2}	9.1 ± 1.4
R115N				
N116L				
T161V				
S283A				
Y323I				
wt human ASL	9.8 ± 0.3	0.40 ± 0.03	32.8 ± 1.0	(8.4 ± 0.7)E^4

[a] Kinetic parameters of wild-type and mutant δ II crystallins as determined by fitting initial velocity data to the Lineweaver−Burk equation.

denaturation/renaturation data was performed by the numerical solver BIOEQS (*44*, *45*). An example of the quality of the fit achieved using this analysis is provided in Figure 3 for the denaturation curve for wild-type δ II crystallin. In all cases the experimental data are very well described by the model, as is evidenced both by the low random residual values (data not shown) and by the low χ^2 for the global fit. The free energies associated the first and second transitions of the denaturation of the wild-type and mutant δ II crystallins have been calculated as the average of the denaturation and renaturation experiments. For wild-type δ II crystallin $\Delta G°_1$, $\Delta G°_2$, and $\Delta G°_{total}$ were calculated to be 16.7 ± 0.2, 47.7 ± 1.7, and 64.5 ± 1.5 kcal/mol^{-1}, respectively. $\Delta G°_{total}$ represents the mean free energy of unfolding for the tetramer ↔ 4 monomer transition. The average values for all mutants and wild-type δ II crystallin were calculated to be 16.6 ± 0.5, 47.2 ± 1.5, 63.8 ± 1.9 kcal mol^{-1} for $\Delta G°_1$, $\Delta G°_2$, and $\Delta G°_{total}$, respectively. These data indicate that wild-type δ II crystallin and its mutants all have similar thermodynamic stabilities. Free energies corresponding to the overall tetramer ↔ monomer transition as well as the individual tetramer ↔ dimer and dimer ↔ monomer transitions were comparable in magnitude for all constructs examined. Reversible denaturation data suggest that the introduction of these mutations into the wild-type δ II sequence does not perturb the thermodynamic stability of the enzyme.

Kinetic Characterization of δ II Mutants. The ASL activity of wild-type and mutant δ II crystallins was quantitated spectrophotometrically by monitoring the appearance of fumarate at 240 nm. All active enzymes displayed linear kinetics, and initial velocity data were fit to the Lineweaver−Burk equation to determine the kinetic parameters K_m and V_{max} (Table 2). Wild-type δ II crystallin has a catalytic efficiency of (7.4 ± 1.8)E^4 M^{-1} s^{-1}, which is comparable to the value observed for wild-type human ASL. The mutations R115N, N116L, T161V, S283A, and Y323I have each abolished ASL activity, while the E296Q mutant has retained only 0.001% residual activity. The kinetic parameters estimated for the E296Q mutant are probably unreliable as its activity is comparable in magnitude to the detection limit of the assay. The S284A and Y323F mutants exhibit catalytic efficiencies which are decreased by an order of magnitude in comparison to wild-type δ II. The remaining mutations appear to have only modest effects on the rate of substrate turnover. It is of interest to note that the Y323F mutant exhibits a K_m value which is increased 24-fold in relation to the wild-type enzyme.

DISCUSSION

Assessment of the Modeling Studies. In this study, modeling was used to identify residues putatively involved in the ASL/δ II crystallin catalytic mechanism. The coordinates of an inhibitor-bound *E. coli* fumarase C structure (*31*) were least-squares superimposed with those of a H110N δ II mutant (Turner and Howell, manuscript in preparation). The argininosuccinate substrate was modeled into the active site, using the position of the citrate inhibitor in the *E. coli* fumarase C active site as a reference for orienting the fumarate moiety of argininosuccinate. The substrate was positioned to lie in an extended conformation across the active site, such that its peptidic end was proximal to H91 (*27*) and its fumarate moiety within hydrogen-bonding distance of H162. Modeling studies allowed for identification of those functional groups which are best positioned to interact with argininosuccinate, and as such these were the most logical targets for site-directed mutagenesis.

Subsequent to the modeling and site-directed mutagenesis studies presented here, the X-ray structure of an inactive H162N δ II crystallin mutant complexed with argininosuccinate was solved using X-ray crystallographic techniques (*1*). This structure allows the validity of the model to be assessed and provides a structural basis for the interpretation of the kinetic data. The kinetic and structural data are in good agreement with one another. Although not correct in all its structural details, the model identified residues H91, R113, S114, R115, N116, V119, T161, T281, N291, D293, E296, Y323, and K325 as being within 8 Å of the substrate. Examination of the crystal structure shows that the model successfully identified approximately half of those residues which make substrate contacts [see Figure 4 (*1*)]. S114, N116, T161, N291, and Y323 interact directly with argininosuccinate, as was predicted by the model, while H91 interacts indirectly via a water molecule with the arginine moiety of the substrate. Residues R113, V119, T281, D293, and K325, which the model suggested might be involved in substrate binding and/or catalysis, do not interact with argininosuccinate. The model failed to identify residues S29, D33, R238, L327, Q328, D330, and K331 as potential substrate binding residues. The roles of these residues in catalysis have not been examined in the current study.

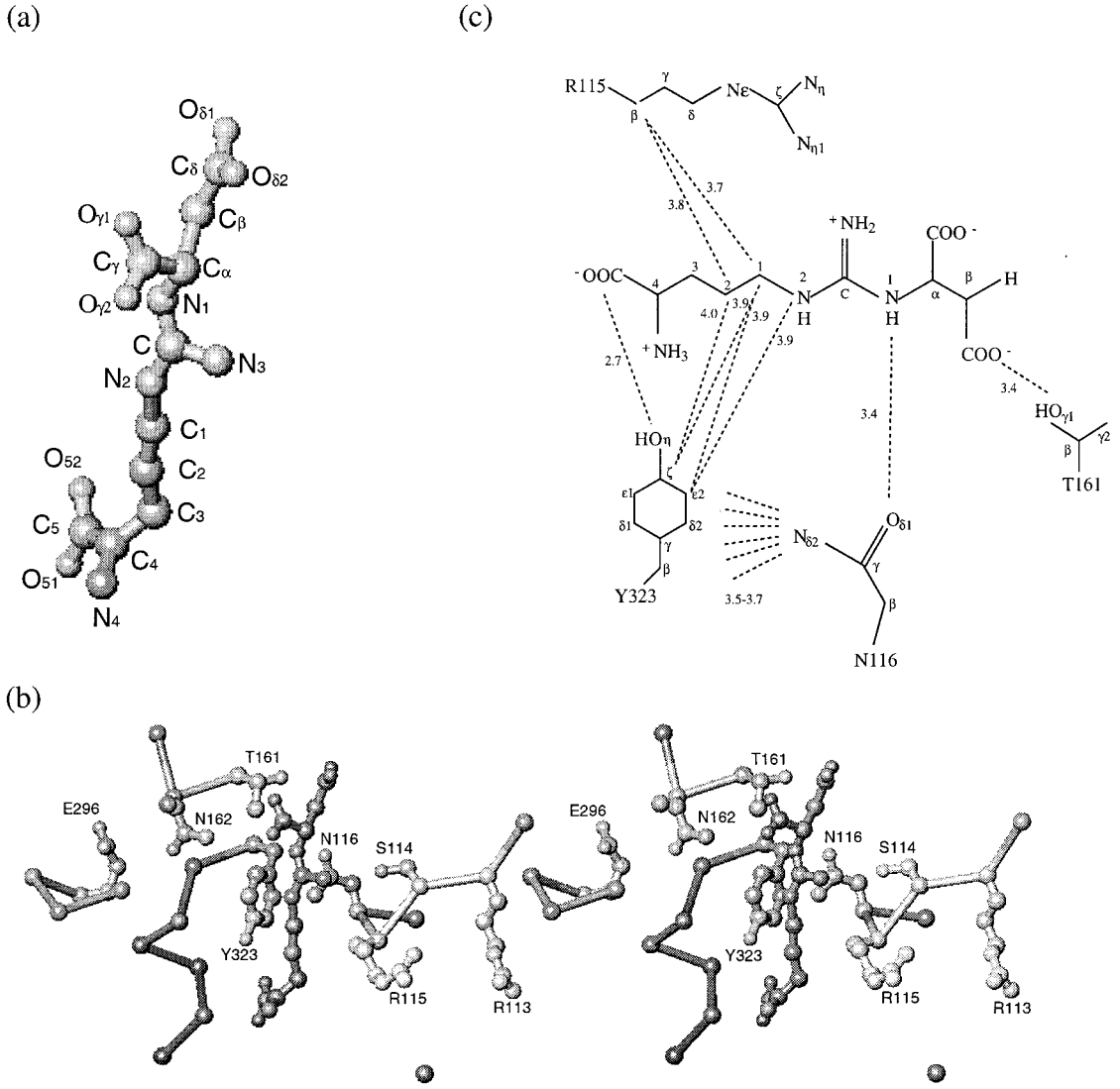

FIGURE 4: (a) Ball-and-stick representation of argininosuccinate, in the same orientation as shown in (b) with the individual atoms labeled. (b) C_α trace (light gray) of the H162N active site (*1*) showing the location of the argininosuccinate substrate (medium gray) and the side chains of protein residues that were mutated. (c) Schematic representation of the interactions between argininosuccinate and four enzymatically important active site residues, Y323, N116, T161, and R115. Dashed lines represent interactions between atoms with distances given in angstroms. Distances are not drawn to scale. The substrate makes additional interactions with active site residues S29, D33, R238, L327, Q328, D330, and K331 [see Table 2 and Figure 4, Vallée et al. (*1*)], which are not shown here.

Circular Dichroism and Reversible Denaturation of δ II Crystallins. Thermodynamic properties were determined for wild-type δ II crystallin and each of its mutants. Gibb's free energies of unfolding/refolding were quantitated in each case in order to verify that changes in kinetic parameters reflected the enzyme's ability to bind or catalyze substrate and were not artifacts of an improperly folded or thermodynamically less stable enzyme. Reversible denaturation of δ II crystallins in GdnHCl revealed that the structural transition from folded tetramer to unfolded monomer occurs via an intermediate species, which has been identified as a dimer from analytical ultracentrifugation experiments performed on human ASL (*43*). Two $\Delta G°$ values can be associated with a biphasic denaturation/renaturation reaction. $\Delta G°_1$ and $\Delta G°_2$ correspond to the tetramer ↔ dimer and dimer ↔ monomer equilibria, respectively. Free energies were determined using the numerical solver BIOEQS (*44, 45*). Wild-type δ II crystallin and its mutants all possess similar thermodynamic stabilities, both for the individual $\Delta G°_1$ and $\Delta G°_2$ transitions and for the overall unfolding/refolding reaction (ΔG_{total}) (data not shown). The free energies of denaturation/renaturation were similar for each of the constructs examined, indicating that the unfolding and refolding reactions occur via the same thermodynamic pathway, i.e., a tetramer ↔ 2 dimer ↔ 4 monomer transition. The thermodynamic data indicate that mutations introduced into the wild-type δ II crystallin coding sequence did not appreciably compromise the thermodynamic stability of the mutants in comparison to wild-type enzyme. In general, the tetramer ↔ dimer and dimer ↔ monomer transitions are associated with free energies of 15−18 kcal mol^{-1} (av 16.6 ± 0.5 kcal mol^{-1}) and 45−50 kcal mol^{-1} (av 47.2 ± 1.5 kcal mol^{-1}), respectively, resulting in an overall tetramer ↔ monomer transition with a free energy of 60−69 kcal/mol^{-1} (av 63.8 ± 1.9 kcal mol^{-1}). On the basis of GdnHCl denaturation data, it was concluded that any differences noted in the kinetic parameters of each mutant directly reflect the enzyme's ability to bind or catalyze the substrate and do not reflect a structurally altered protein.

The superposition of circular dichroism spectra (Figure 2) of wild-type and mutant δ II crystallins revealed that, with

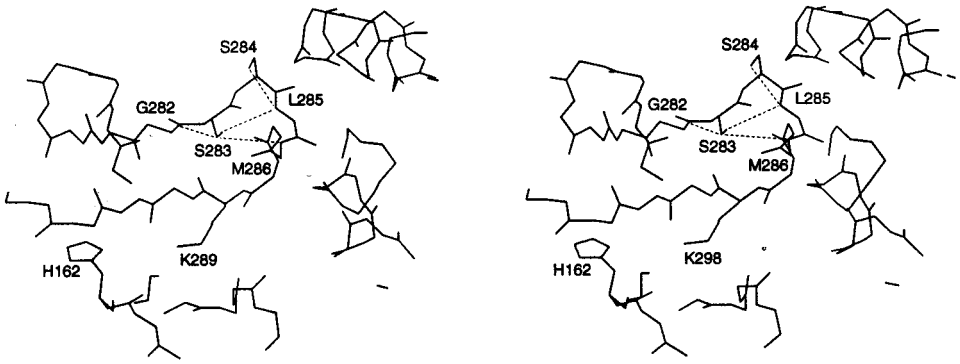

FIGURE 5: Stereoview of the H110N δ II crystallin active site showing the location of residues S283 and S284 in relation to K289 and H162.

the exception of R115N and E296Q, the introduction of a mutation did not perturb the secondary structural elements of the constructs examined. Differences in the spectra of R115N and E296Q may be due to errors in protein concentration, which could arise from the presence of impurities or small aggregates in the assay solution. If, however, these differences are real, the data are indicating that the R115N and E296Q mutants have lost 20−30% of their α-helicity in relation to wild-type δ II crystallin. It is of interest to note that the R115N and E296Q mutations are at the beginning of helices h7 and h12 of domain 2, respectively [see Figure 1c (*1*)]. This domain is responsible for the oligomerization of the protein and forms the 20-helix core of the tetrameric enzyme (*27*). On the basis of their locations in α-helices, the mutation of R115 and E296, although unlikely, could destabilize these constructs, resulting in an altered conformation and hence different CD spectra. In general, both the thermodynamic and circular dichroism spectra are in good agreement and consistent with the idea that the kinetic parameters measured reflect the enzyme's ability to catalyze the substrate.

Roles of Active Site Residues in Catalysis. The kinetic data (Table 2) show that although wild-type duck δ II crystallin and human ASL have different V_{max} and K_m values, they still have comparable catalytic efficiencies, $(7.4 \pm 1.8)E^4$ M^{-1} s^{-1} and $(8.4 \pm 0.7)E^4$ M^{-1} s^{-1}, respectively. The S114A and R113N mutants both exhibit catalytic efficiencies that are similar in magnitude to wild-type ASL/δ II crystallin and as such are unlikely to participate directly in the catalytic mechanism. These data preclude the possibility of S114 functioning as a hydrogen ion donor, as had previously been suggested in the context of *E. coli* fumarase C (*30*). The X-ray data also indicate that S114 is not a catalytic residue, as its $O_{\gamma 1}$ is positioned 4.1 Å from the guanidinium group of argininosuccinate. R113 does not make any contacts with argininosuccinate. Its $N_{\eta 2}$ moiety lies approximately 12 Å from the C_1, C_2, and C_3 backbone atoms of the substrate.

The roles of six functional groups, Y323, R115, T161, S283, E296, and N116, each of which abolished activity when mutated, can be explained in light of the X-ray data (Figure 4). In the case of Y323, the two mutations Y323I and Y323F each produce different kinetic results which can be explained from the known protein−substrate contacts. The Y323F mutant exhibited a catalytic efficiency that is decreased by an order of magnitude in comparison to wild-type δ II crystallin [$(2.5 \pm 0.1)E^3$ M^{-1} s^{-1} vs $(7.4 \pm 1.8)E^4$ M^{-1} s^{-1}]. The H162N crystal structure shows that the Y323's hydroxyl moiety is within hydrogen-bonding distance (2.7 Å) of the carboxyl oxygen of the peptidic end of the substrate molecule. Removal of the hydroxyl group impairs binding, as is evidenced by the 24-fold increase in K_m (1.7 ± 0.1 mM) relative to that of the wild-type protein (0.07 ± 0.01 mM). The V_{max} of the Y323F mutant (1.3 ± 0.1 μmol min^{-1} mg^{-1}) is comparable to that of wild-type (1.5 ± 0.2 μmol min^{-1} mg^{-1}), with the net effect being a catalytic efficiency that is reduced by an order of magnitude in relation to the wild-type enzyme. In contrast, the Y323I mutation completely abolishes detectable ASL activity, illustrating that the phenyl group is a greater binding determinant than the hydroxyl moiety. The structure reveals the potential for van der Waal interactions between C_ζ and $C_{\epsilon 2}$ ring members of Y323 and the C_1, C_2, and N_2 atoms of the substrate (3.7−4.0 Å). These interactions would be lost in the Y323I mutant.

The loss of activity upon mutation of R115 may be attributed to assigning it a substrate binding role, as this residue makes hydrophobic interactions with the arginine backbone of argininosuccinate. The C_β of R115 is positioned 3.8 and 3.7 Å from the C_2 and C_1 atoms of argininosuccinate, respectively, suggesting that it may play a role in stabilizing its flexible tail. R115 is also positioned to interact with H91. The C_δ, C_ζ, and N_ϵ atoms make contacts (3.1−3.9 Å) with members of the imidazole ring and C_β atom of H91. R115 may therefore participate in correctly positioning H91 for its putative substrate binding role. H91 interacts with the arginine moiety of the substrate via a water molecule, and mutation of this residue to glutamine or asparagine results in a reduction of the activity to 10% of that of wild type (*27*, *34*). It is difficult to rationalize why H91 should have such a major effect on catalysis, given that its interaction with the substrate is not direct. T161 also interacts with argininosuccinate $O_{\delta 1}$ (3.4 Å), and therefore the T161V mutation presumably exerts its effect either by altering the conformation of the adjacent H162 or by affecting protein−substrate interaction, either of which would prevent substrate turnover and account for the inactivity of this mutant.

Unlike the other residues examined, S283 and S284 are relatively remote from the site of substrate binding (8.6 and 12.3 Å, respectively, from the C_α of argininosuccinate) (Figure 5). Both of these residues are invariant across ASL/δ crystallin superfamily members and are located on a conformationally flexible loop (the 280's loop) close to the active site cleft. While the S283A mutation completely inhibits catalysis, the S284A mutant exhibited activity that was an order of magnitude less than that of the wild-type enzyme

$(5.3 \pm 0.6)E^3\ M^{-1}\ s^{-1}$ vs $(7.4 \pm 1.8)E^4\ M^{-1}\ s^{-1}$, respectively. The functions of S283 and S284 remain unknown but are likely to be structural rather than catalytic in nature. The mutations may affect the flexibility of the 280's loop and therefore the position of K289, which is the only charged amino acid that is absolutely conserved across all superfamily members. K289 is speculated to help stabilize the carbanion intermediate that is formed during hydrolysis. The importance of this residue in catalysis has been demonstrated in *E. coli* L-aspartase, in which a K289R mutant retained only 0.3% of wild-type activity (*46*). Examination of an H110N δ II crystallin mutant structure, in which the 280's loop can be seen (Turner and Howell, manuscript in preparation), reveals that the side-chain atoms of S283 and S284 are primarily involved in local contacts with the backbone atoms of adjacent residues G282, L285, and M286. The disruption of these interactions may account for the inactivity of the S283 mutant, in which the loss of backbone stability could cause a conformational change in the 280's loop and a relocation of K289.

The kinetics displayed by the E296Q mutant supports the hypothesis that this residue participates in a charge-relay system with H162 (*30*). The E296Q mutant displays a catalytic efficiency that is 4 orders of magnitude less than that of wild-type δ II crystallin. Disrupting the charge-relay would drastically diminish the proton-withdrawing abilities of H162, resulting in only residual levels of catalytic activity. Unlike the structural data available for *E. coli* fumarase C, which implicates an active site water molecule as the catalytic base, there is no evidence of the presence of an analogous water molecule in the structure of either mutant δ II crystallins (*1*, *27*) or wild-type human ASL (*29*). Current evidence would suggest that, in the catalytic mechanism of ASL/δ II crystallin, H162 acts directly as the catalytic base rather than exerting its effect by activating a water molecule.

The N116L mutant retained no detectable ASL/δ II crystallin catalytic activity. This residue is located in the first of the three highly conserved regions (Figure 1). On the basis of its position relative to the substrate, we propose that N116 plays a role in substrate binding. N116 $O_{\delta 1}$ is located 3.4 Å from the argininosuccinate N_1 while the N116 $N_{\delta 2}$ makes π interactions with every atom of Y323's phenyl group (3.5−3.7 Å), suggesting that this residue also helps position Y323 for its substrate binding role. N116 in the δ II active site is superimposable with the analogous residue in inhibitor-bound *E. coli* fumarase C (*31*). In the latter structure, N116 $N_{\delta 2}$ is positioned 3.0 Å from the O_3 of the citrate inhibitor molecule. While N116 is positioned 3.4 Å from the scissle bond of argininosuccinate that is cleaved during the enzymatic mechanism, the asparagine is unlikely to function as the catalytic acid. N116 does not interact with other active site residues, and therefore N116 could be responsible for positioning a water molecule, perhaps the same water that has been suggested to be involved in the catalytic mechanism of *E. coli* fumarase C (*31*). To date, there is no crystallographic evidence to support the involvement of water in the catalytic mechanism of ASL/δ II crystallin, and therefore the identity of the catalytic acid remains undetermined.

The kinetic results presented here are in good agreement with the X-ray data. Together they provide us with a more thorough understanding of the manner in which δ II crystallin binds and hydrolyzes its argininosuccinate substrate, although the identity of the catalytic acid remains undetermined.

ACKNOWLEDGMENT

The authors thank Dr. Bill O'Brien for supplying the pET expression system for wild-type δ II crystallin and Patrick Yip for constructing the histidine-tagged expression system.

REFERENCES

1. Vallee, F., Turner, M. A., Lindley, P. L., and Howell, P. L. (1999) *Biochemistry 38*, 2425−2434.
2. Piatigorsky, J. (1989) *Faseb J. 3*, 1933−1940.
3. Piatigorsky, J. (1984) *Cell 38*, 620−621.
4. Wistow, G. J., and Piatigorsky, J. (1988) *Annu. Rev. Biochem. 57*, 479−504.
5. Delaye, M., and Tardieu, A. (1983) *Nature 302*, 415−417.
6. Fernald, R., and Wright, S. (1983) *Nature 301*, 618−620.
7. Riddihough, G. (1994) *Nature 371*, 538.
8. Wistow, G. (1993) *Trends Biochem. Sci. 18*, 301−306.
9. Piatigorsky, J. (1992) *J. Biol. Chem. 267*, 4277−4280.
10. Wistow, G., and Piatigorsky, J. (1987) *Science 236*, 1554−1556.
11. Piatigorsky, J., and Wistow, G. J. (1989) *Cell 57*, 197−199.
12. Piatigorsky, J., O'Brien, W. E., Norman, B. L., Kalumuck, K., Wistow, G. J., Borras, T., Nickerson, J. M., and Wawrousek, E. F. (1988) *Proc. Natl. Acad. Sci. U.S.A. 85*, 3479−83.
13. Piatigorsky, J., Kantorow, M., Gopal-Srivasta, R., and Tomarev, S. (1994) in *Toward a Molecular Basis of Alcohol Use and Abuse* (Jansson, B., Jornvall, H., Rydberg, U., Terenius, L., and Vallee, B., Eds.) Birkhauser Verlag, Basel, Switzerland.
14. Hughes, A. (1994) *Proc. R. Soc. London, Ser. B 256*, 119−124.
15. Kimura, M., and Ota, T. (1974) *Proc. Natl. Acad. Sci. U.S.A. 71*, 2848−2852.
16. Piatigorsky, J., and Wistow, G. (1991) *Science 252*, 1078−1079.
17. Blundell, T., Lindley, P., Miller, L., Moss, D., Slingsby, C., Tickle, I., Turnell, B., and Wistow, G. (1981) *Nature 289*, 771−777.
18. Simpson, A., Bateman, O., Driessen, H., Lindley, P., Moss, D., Mylvaganam, S., Narebor, E., and Slingsby, C. (1994) *Nat. Struct. Biol. 1*, 724−734.
19. Mori, M., Matsubasa, T., Amaya, Y., and Takiguchi, M. (1990) *Prog. Clin. Biol. Res. 344*, 683−699.
20. O'Brien, W. E., McInnes, R., Kalumuck, K., and Adcock, M. (1986) *Proc. Natl. Acad. Sci. U.S.A. 83*, 7211−7215.
21. O'Brien, W. E., and Barr, R. H. (1981) *Biochemistry 20*, 2056−2060.
22. Woods, S. A., Schwartzbach, S. D., and Guest, J. R. (1988) *Biochim. Biophys. Acta 954*, 14−26.
23. Woods, S. A., Miles, J. S., Roberts, R. E., and Guest, J. R. (1986) *Biochem. J. 237*, 547−557.
24. Takagi, J. S., Tokushige, M., Shimura, Y., and Kanehisa, M. (1986) *Biochem. Biophys. Res. Commun. 138*, 568−572.
25. Stone, R. L., Zalkin, H., and Dixon, J. E. (1993) *J. Biol. Chem. 268*, 19710−6.
26. Williams, S. E., Woolridge, E. M., Ransom, S. C., Landro, J. A., Babbitt, P. C., and Kozarich, J. W. (1992) *Biochemistry 31*, 9768−9776.
27. Abu-Abed, M., Turner, M. A., Vallee, F., Simpson, A., Slingsby, C., and Howell, P. L. (1997) *Biochemistry 36*, 14012−14022.
28. Shi, W., Dunbar, J., Jayasekera, M. M., Viola, R. E., and Farber, G. K. (1997) *Biochemistry 36*, 9136−9144.
29. Turner, M. A., Simpson, A., McInnes, R. R., and Howell, P. L. (1997) *Proc. Natl. Acad. Sci. U.S.A. 94*, 9063−9068.
30. Weaver, T. M., Levitt, D. G., Donnelly, M. I., Stevens, P. P., and Banaszak, L. J. (1995) *Nat. Struct. Biol. 2*, 654−662.
31. Weaver, T., and Banaszak, L. (1996) *Biochemistry 35*, 13955−13965.
32. Lee, H. J., Chiou, S. H., and Chang, G. G. (1993) *Biochem. J. 293*, 537−544.

33. Garrard, L. J., Bui, Q. T., Nygaard, R., and Raushel, F. M. (1985) *J. Biol. Chem. 260*, 5548−5553.
34. Patejunas, G., Barbosa, P., Lacombe, M., and O'Brien, W. E. (1995) *Exp. Eye Res. 61*, 151−154.
35. Kleywegt, G. (1996) *Acta Crystallogr. B52*, 842−857.
36. Kleywegt, G. J., and Jones, T. A. (1996) *Structure 4*, 1395−1400.
37. Kleywegt, G. J., and Jones, T. A. (1995) *Structure 3*, 535−540.
38. QUANTA (1996) Molecular Simulations Inc., Waltham, MA.
39. Roussel, A., Inisan, A.-G., and Cambillau, C. (1991) *Silicon graphics geometry partners directory*, Mountain View, CA.
40. Conley, E. C., and Saunders, J. R. (1984) *Mol. Gen. Genet. 194*, 211−218.
41. Deng, W. P., and Nickoloff, J. A. (1992) *Anal. Biochem. 200*, 81−88.
42. Sambrook, J., Fritsch, E., and Maniatis, T. (1989) *Molecular Cloning: A Laboratory Manual*, Cold Spring Harbor Laboratory, Cold Spring Harbor, NY.
43. Thompson, G. (1998) MSc. Thesis, University of Toronto.
44. Royer, C. A., and Beechem, J. M. (1992) *Methods Enzymol. 210*, 481−505.
45. Royer, C. A. (1993) *Anal. Biochem. 210*, 91−97.
46. Saribas, A. S., Schindler, J. F., and Viola, R. E. (1994) *J. Biol. Chem. 269*, 6313−6319.

BI982150G